THE BALTIC JOURNAL
OF ROAD
AND BRIDGE
ENGINEERING
2020/15(5)

ISSN 1822-427X/eISSN 1822-4288
2020 Volume 15 Issue 5: 136–159
https://doi.org/10.7250/bjrbe.2020-15.511

DETERMINING SOIL MOISTURE CONTENT AND MATERIAL PROPERTIES WITH DYNAMIC CONE PENETROMETER

JUHA LATVALA[1*], HEIKKI LUOMALA[2], PAULI KOLISOJA[3]

[1–3]*Research Centre Terra, Tampere University, Tampere, Finland*

Received 21 October 2019; accepted 12 May 2020

Abstract. This study utilised static triaxial and dynamic cone penetration tests to examine the identification of changes in strength in soil materials as a result of an increase in moisture content. The applicability of a light dynamic cone penetrometer device in railway environments was also studied. On a broader scale, the aim was to find an investigation method suited to field locations that identify low-quality or persistently moist materials directly from the structure. The triaxial tests found an apparent increase in shear strength when the water content dropped below 7%. Based on the series of laboratory tests, the dynamic cone penetrometer reacted strongly to material density, but the impact of moisture content was also evident. Furthermore, the results showed that dynamic cone resistance is a reasonably unfeasible metric for assessing the structural quality of materials consisting primarily of sand, due to the number of factors affecting the resistance. In the laboratory tests, the lowest dynamic cone resistances were measured in the material with the highest structural quality.

Keywords: dynamic cone penetrometer (DCP), Panda2, railway embankments, soil moisture, soil shear strength, substructure, triaxial test.

* Corresponding author. E-mail: juha.latvala@tuni.fi

Juha LATVALA (ORCID ID 0000-0001-6306-9310)
Heikki LUOMALA (ORCID ID 0000-0002-7113-3527)
Pauli KOLISOJA (ORCID ID 0000-0001-7709-180X)

Introduction

In the future, climate change is predicted to steer the global climate towards extreme phenomena, leading to increasingly frequent floods, heavy rains and, in some locations, extreme drought (Trenberth, 2011). In Finland, this shift is expected to increase annual rainfall by multiple percentage points, depending on the method of calculation (Ruosteenoja, Jylhä, & Kämäräinen, 2016). The intensity of individual instances of rainfall is also predicted to increase (Lehtonen, 2011). Increased moisture content is known to deteriorate the functionality of earth structures. As reported by Li & Selig (1995), the combination of cyclic loading, fine-grained soils, and excessive moisture content is a very harmful combination for a railway track. Thus, climate change exposes earth structures to accelerated deterioration. The Finnish Transport Infrastructure Agency and Tampere University have initiated a research project that examines the effect of moisture conditions on the bearing capacity of track earth structures and the possible benefits obtainable by drainage. One goal of the research efforts is to develop the field testing of soil materials and the identification of low-grade substructure materials. The suitable in-situ test methods vary depending on soil type. For sandy materials, Selig & Waters (1994) have listed functional methods such as standard penetration test (SPT), cone penetration test (CPT), borehole shear test (BST) and dilatometer test (DMT). One of the easiest and lightest to operate is the dynamic cone penetrometer (DCP).

Brough, Ghataora, Stirling, Madelin, Rogers, & Chapman (2003) have also been interested in track subgrade quality in their research (part 1/2) because they assumed a relationship between track-bed stiffness and track quality deterioration. Dynamic cone penetrometer was identified as one potential tool for determining the bearing capacity of subgrade. After a case study (part 2/2), Brough, Ghataora, Stirling, Madelin, Rogers, & Chapman (2006) considered that DCP is suitable for recognising subgrade heterogeneity at least. Kennedy (2011) has also mentioned DCP as a potential in-situ testing device for railway track substructures and recommends further research because there is some scatter in the results of DCP. In this study, the Panda2, which is a light hand-operated DCP manufactured by the French company Sol Solution, was selected as one of the potential examination methods. The device measures the dynamic cone resistance of the auger rod in proportion to depth, based on the stroke intensity and rod penetration. The Panda2 records the measurements automatically and enables them to be exported to a computer. The benefits of the device include ease of use and compact size. In light of the research project as a whole, the following research questions were identified:

1. Is dynamic cone resistance measured by the DCP suitable quantity to identify materials that have low bearing capacity?
2. Is the DCP accurate enough to detect changes in strength resulting from the changes in the moisture content of materials?
3. Is a light hand-operated DCP practically feasible for the Finnish railway environment?

Answers to the research questions were sought through an extensive series of laboratory tests and field measurements. Static triaxial tests were conducted on the materials being studied at varying moisture content levels to determine the impact of moisture, and the results were compared to the DCP measurement results.

1. Theoretical framework

Various penetrometers have been used in soil surveys for quite some time, and the method is regarded as the oldest geotechnical in-situ test (Spagnoli, 2007). As reported by Vanags, Minasny, & McBratney (2004), Parker & Jenny (1945) were the first to introduce a precursor to the DCP. In their tests, they measured the energy required to drive a test pipe into the soil by using a 9.1 kg weight dropped from a height of 30 cm and measuring the pipe penetration per stroke. This technique revealed the soil resistance in Joules per centimetre. The development of the method

Figure 1. The Panda2 device

continued, and the modern penetrometer was introduced in studies by the Australian engineer Scala (1956). Panda2 device by Soil Solution Ltd is a further developed version of the penetrometer that works with variable impact strength as it also measured. The French scientist Dr Roland Gourves of Blaise Pascal University has been developing Panda since 1991 (Langton, 1999).

Langton (1999) described the operating principle of the device in a technical article. Figure 1 presents the device in working order at a field location. The Panda2 device generates the impact energy using a recoil-free hammer and measures it with a connecting piece attached to the top end of the rod. The penetration of the cone-tipped rod into the soil is measured automatically with a self-spooling measuring tape attached to the connecting piece at the top of the rod. The connecting piece features an acceleration sensor that determines the impact speed. The terminal device records the results. The weight of the recoil-free hammer used in the Panda is 2.0 kg.

As reported by Langton (1999), the q_d is calculated using the "Dutch formula", which has been modified from the original form presented by Cassan 1988 (as cited in Langton, 1999). The calculation of q_d is based on the following equation:

$$q_d = \frac{1}{A} \cdot \frac{0.5\ MV^2}{1+\frac{P}{M}} \cdot \frac{1}{x_{90°}},$$

where q_d – dynamic cone resistance; $x_{90°}$ – penetration caused by a single strike with a 90° cone; A – cone area; M – weight of the striking mass; P – weight of the struck mass; V – impact speed of the hammer.

The variables contained by the formula indicate that it does not account for the skin resistance between the rod and the soil. A third version of the device is also under development, which measures more parameters but also assumes the skin resistance to be zero (Benz-Navarrete, Escobar, Haddani, Gourves, D'Aguiar, & Calon, 2014). The diameters of the cones used at the end of the rod vary. The device uses a fixed 2 cm^2 cone or a larger 4 cm^2 sacrificial cone. The diameters of these cones are 16 mm and 22.5 mm, respectively. The diameter of the impact rods is 14 mm, and the length of a single section is 500 mm. The article written by Langton (1999) also mentions a 10 cm^2 cone for special cases. The angle for all cone pieces is 90°. The Panda2 device typically measures 20–30 MPa dynamic cone resistance to an approximate depth of 4–6 m. In favourable conditions, the device measures to even deeper. The dynamic cone resistance q_d is used directly in the monitoring of compaction and in soil surveys. As reported by Langton (1999), the link between dynamic cone resistance and other commonly-used parameters have been studied using a variety of well-documented test sites where

studies have been conducted using a range of methods. The commonly-used comparable parameters in those studies were SPT and other types of DCP, California Bearing Ratio (CBR) measurements and undrained shear strength.

2. Materials and methods

2.1. Materials

The laboratory tests were carried out with four different materials, for which the particle size distributions and typical geotechnical parameters are presented in Figure 2 and Table 1, respectively. Screened sand from the Kollola gravel pit, which meets the requirements of the Finnish Transport Infrastructure Agency for insulation and intermediate layer materials, was used as high-quality reference material. The three others were actual samples from the Rantarata track in southern Finland, only one of which (km44) fulfilled the particle size requirements. The field samples deviate from the reference materials mainly concerning the fine-grained end, as the reference material

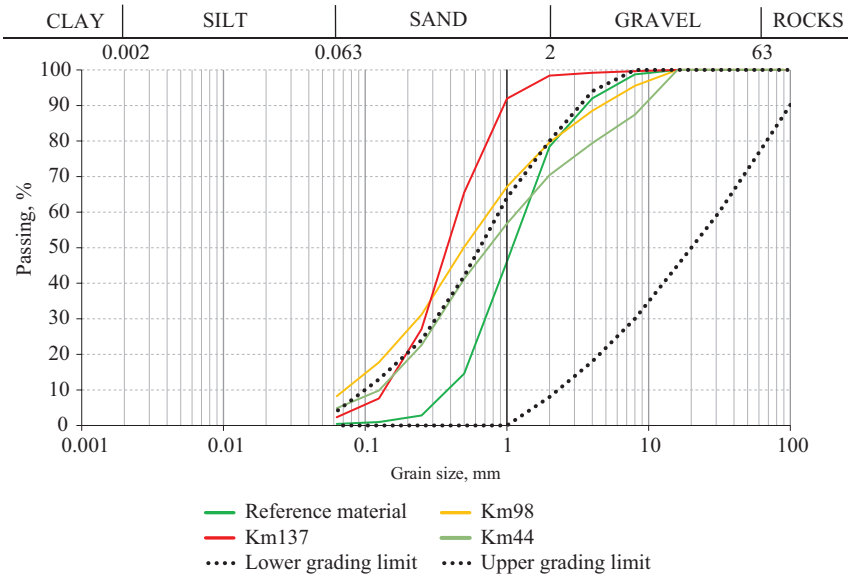

Note: the particle size limits of the Finnish Transport infrastructure Agency for insulation and intermediate layer materials are illustrated with dotted lines.

Figure 2. Particle sizes of the materials used in the laboratory tests

Table 1. Geotechnical properties of the studied materials

Material	Particle size ratio		Fine fraction content diameter below	Dry density and water content (Wet samples, Proctor)	Dry density (Dry samples, Proctor)
	d_{50}, mm	d_{60}/d_{10}, -	0.06 mm, %	ρ_{dmax}, g/cm^3 and %	ρ_{dmax}, g/cm^3
Reference material	1.20	3.75	0	1.91/2.80	1.96
km44	0.75	9.60	4.90	2.03/8.50	2.10
km98	0.50	10.70	8.20	2.14/3.00	2.08
km137	0.40	3.60	2.30	1.80/5.90	1.90

consisted of screened 0/8 mm sand, whereas the field material contained fines. The largest deviation from the guideline range was presented by the material km137, which was excessively even-grained, resulting in low compaction properties.

For laboratory testing, the compaction behaviour of the materials was studied with the improved Proctor test method (*SFS-EN 13286-2:2011 Unbound and Hydraulically Bound Mixtures. Part 2: Test*

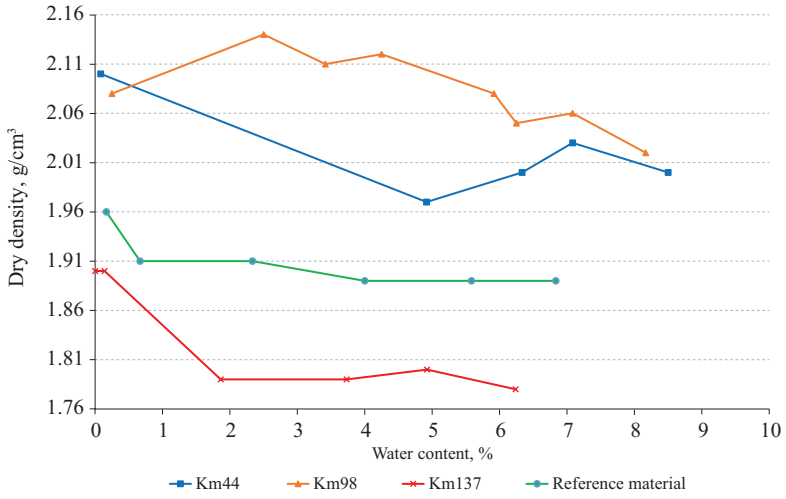

Figure 3. Results of the improved Proctor tests for the studied materials

Methods for Laboratory Reference Density and Water Content. Proctor Compaction). The test results are presented in Figure 3 and Table 1. The best compaction results were obtained with the km98 material, with a peak dry density of 2.14 g/cm^3 at a compaction water content of 3%. km44 material reached its highest dry density as oven-dried and the second-highest dry density at a moisture content of 8.5%. The reference material and the km137 sample were looser (1.96 g/cm^3 and 1.90 g/cm^3), and for them, too, the maximum density was achieved with an oven-dry sample. The compaction curve for the reference material, in particular, shows that when the material is moist, the maximum dry density remains relatively constant across a broad moisture content range.

2.2. Static triaxial tests

The materials being studied have been subjected to a series of dried triaxial tests to determine the impact of moisture content on the maximum shear strength. The saturated samples were prepared by the *SFS-ISO 17892-9:2018 Geotechnical Investigation and Testing. Laboratory Testing of Soil. Part 9: Consolidated Triaxial Compression Tests on Water Saturated Soils* standard, with the exception that saturation ratio was not confirmed through the B value. The samples were first compacted at near optimum moisture content – 4.1–8.7%,

Table 2. Parameters used in the triaxial and measured material properties

The sample ID	Cell pressure, kPa	Moisture condition/ drying procedure	Water content during compaction, %	Dry density after compaction/ consolidation, g/cm^3	Water content after test, %	Maximum shear stress, kPa
			km44			
A1	21.0	Saturated	6.20	1.96/1.96	11.50	90
B1*1	41.0	Saturated	7.00	1.96/1.97	11.40	138
B2	41.0	Saturated	6.40	1.96/1.96	11.40	160
C1	81.0	Saturated	8.10	1.93/1.95	11.00	245
D1	41.0	1 d: -4.0 kPa	7.30	1.94/1.94	9.70	138
E1	39.0	3 d: -4.0 kPa	7.40	1.92/1.92	6.80	138
F1	41.0	5 d: -4.0 kPa	7.40	1.91/1.95	5.50	175
G1	41.0	10 d: -4.0 kPa	8.70	1.92/1.93	0.30	295
H1	41.0	7 d: -4.0 kPa	4.90	1.93/1.94	5.00	165
I1	41.0	3.25 d: -5.0 kPa	4.10	1.94/1.95	2.60	205

Table 2.

The sample ID	Cell pressure, kPa	Moisture condition/ drying procedure	Water content during compaction, %	Dry density after compaction/ consolidation, g/cm^3	Water content after test, %	Maximum shear stress, kPa
			km98			
A1	19.0	Saturated	5.60	2.00/2.00	11.40	90
B	41.5	Saturated	5.80	1.99/2.00	11.00	160
C1	82.0	Saturated	5.60	2.02/2.03	11.20	360
C2	82.0	Saturated	6.00	2.01/2.02	10.80	285
DA	40.0	1d: -5.0 kPa	5.80	1.98/2.00	7.40	170
E	41.0	3d: -5.0 kPa	5.50	2.00/2.01	6.00	180
F	41.0	5 d: -5.0 kPa	5.10	2.03/2.04	3.70	260
			km137			
A2	20.0	Saturated	6.10	1.79/1.79	14.40	70
B	41.0	Saturated	6.30	1.79/1.79	14.90	145
C	81.0	Saturated	6.60	1.80/1.81	14.60	270
D	41.0	1 d: -5.0 kPa	5.80	1.77/1.80	4.30	150
E	40.0	3 d: -5.0 kPa	6.30	1.79/1.80	0.20	280
F	41.0	5 d: -5.0 kPa	6.40	1.80/1.79	7.50	145
U	41.0	2 d: -5.0 kPa	5.30	1.78/1.79	0.70	230
U1	41.0	2 d: -4.5 kPa	7.60	1.82/1.87	3.20	180
			Reference material			
A	19.5	Saturated	5.70	1.93/1.93	12.80	130
B1	40.0	Saturated	7.10	1.96/1.96	12.50	220
C	80.5	Saturated	6.30	1.97/1.99	11.11	410
D	40.5	1 d: -3.5 kPa	7.00	1.93/1.95	5.70	220
E	40.5	3 d: -4.5 kPa	6.20	1.93/1.95	0.30	415
F	40.0	3 d: -3.0 kPa	6.50	1.92/1.93	0.70	380
G	39.0	n. 1 d: -4.0 kPa	6.10	1.95/1.96	4.70	250

Note: *1 B1 test was repeated with B2 because dry density was above the average.

depending on the material – to obtain samples with identical densities. After this, the samples were saturated and consolidated. Following the consolidation, the air was sucked through each sample at a negative pressure of 3.5–5.0 kPa to dry the samples. The drying time and vacuum level were varied to achieve a range of different moisture contents. The values used in the tests are presented in Table 2. The

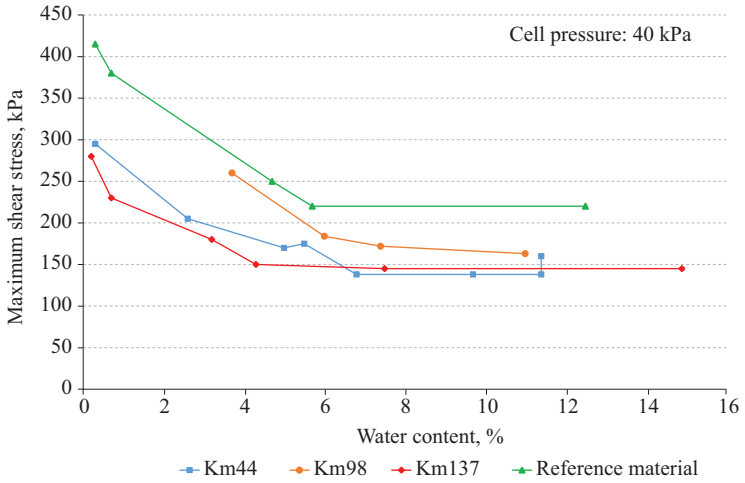

Figure 4. The achieved maximum shear stresses of the static triaxial tests at varying moisture content levels

Table 3. Parameters used in the triaxial and measured material properties

Sample ID	Cohesion, kPa	Friction angle, °	Cohesion after failure, kPa	Friction angle after failure °	Strain level at maximum shear stress, %
km98	10.9	49.4	4.8	38.6	
A1					1.00
B					1.80
C2					2.60
km44	18.8	45.6	3.9	39.1	
A1					1.20
B2					1.30
C1					1.70
km137	4.1	49.5	6.1	37.2	
A2					2.80
B					2.40
C					2.40
Reference material	10.2	55.4	9.6	40.2	
A					2.60
B1					2.30
C					3.10

maximum shear stresses at a cell pressure of 40 kPa were compiled into Figure 4. The results suggest that the maximum shear strength begins to increase when the moisture content of the studied materials is below 7%. There are, however, differences among the materials, since with km44 material the growth starts at a moisture content of 6.8%, whereas with km137 material it starts at below 4.3%. With the same material, the increase in shear strength is significant, and the difference between relatively moist and relatively dry samples is above 100 kPa. For saturated samples, the friction angles and cohesion values measured at different cell pressures are presented in Table 3. The friction angles and cohesions from saturated tests are relatively small compared to the shear strengths achieved with drier samples. That means that there is an influence of apparent cohesion component, adding the shear strength. The results of the triaxial tests indicate that reducing the moisture content substantially increases the shear strength of the soil.

2.3. Methods

In the laboratory, the functionality of the Panda2 device was examined using soil samples contained in plastic tubes. The interior diameter of the pipes was 235 mm, and their height was 800 mm. The bottom of each pipe was closed with a plug, which had holes for saturation and drainage. The bottom plug was covered with geotextile and a perforated plywood board for the bottom contact of the DCP rod. All material samples were compacted at the same moisture content, and the compaction procedure was kept constant. After the compaction, the samples were saturated and dried to achieve a variety of moisture contents. In the layered compaction, an efficient vibratory hammer was used for which a 200 mm diameter compaction plate had been manufactured. Figure 5 depicts an on-going measurement process from the laboratory. A unit that measures device depth is positioned at the top of the sample, and a sensor measuring impact force is visible at the end of the penetrometer rod. The samples were prepared by the following process:

1. A concrete mixer is used to moisten the dry material to a moisture content of 7–8%, i.e. near to the optimum water content.
2. A known amount of material is poured into the sample tube, resulting in a layer of approximately 50 mm after compaction.
3. The sample in the tube is compacted with a vibrating compactor. A constant compaction time of 30 s was used for each layer.
4. More sample material is added until the target sample height is reached.

Figure 5. Panda2 test in progress in the laboratory

5. The compacted sample is moistened with water until it is close to the saturated state. The sample is moistened either from the top only or from the top and bottom simultaneously.
6. The sample is permitted to dry at room temperature for the duration specified in the test programme.
7. The Panda2 device is used to drive three or four penetrometer rods into the sample.
8. The sample is dismantled in layers of 100 mm. The layers are weighed, dried and weighed again to determine the moisture content of each portion.

3. Results

In the data directly recorded by the device, the dynamic cone resistances generated by individual impacts vary significantly due to the heterogenic properties of the soil. For this reason, the results presented here have been calculated as averages of the three rods driven into each sample, for one 100 mm section at a time. For almost all materials, the highest dynamic cone resistance was achieved at a depth of 400–500 mm. After that depth, the resistance usually began to decrease. The phenomenon was studied with a static penetrometer test, in which a computer-controlled hydraulic jack was used to drive the rod of the

Panda2 device into the sample at a constant speed. The force required for penetration was measured. The phenomenon of the dynamic cone resistance decreasing over the final 200 mm was also evident in this test, which implies that the effect is caused by skin resistance or the loosening of the base layers during the compaction of the upper layers. Therefore, the averages of dynamic cone resistance were primarily examined across the depths of 0–500 mm.

One series of tests was conducted with oven-dry materials. The oven-dry samples were prepared differently from the others in that they were compacted dry, which led to varying dry densities. The test results are shown in Figure 6, which specifies the average dynamic cone resistance of the three driven rods to depth. The results show that the measured dynamic cone resistance of all materials increases dramatically in proportion to the depth and that the highest value is achieved at an approximate depth of 450 mm. The dynamic cone resistance correlates strongly with the dry density of the samples, as km44 (2.23 g/cm^3) and km98 (2.18 g/cm^3) were denser than km137 (-g/cm^3) and reference material (1.87 g/cm^3). With dry material, the median particle size does not appear to be a significant parameter in the particle size range of the materials examined based on the similarity of the curves, since the values for the km137 and reference materials were 0.4 mm and 1.2 mm, respectively.

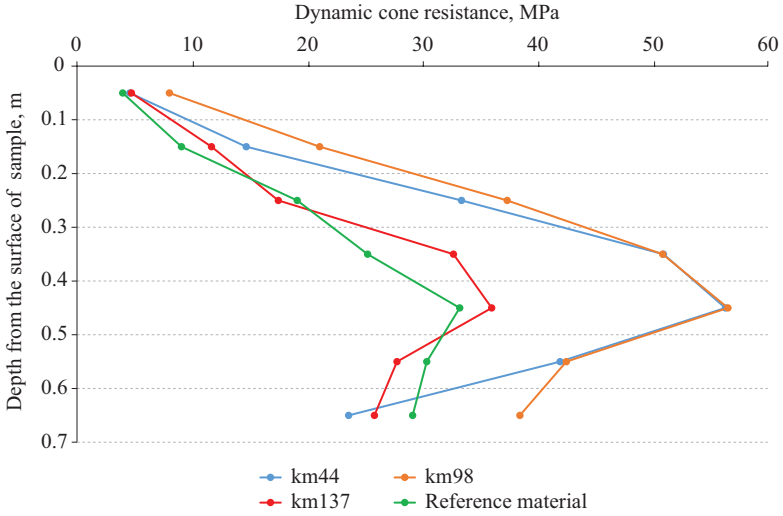

Note: the results are averages of three tests across layers of 100 mm.

Figure 6. Dynamic cone resistance measured with oven-dry samples

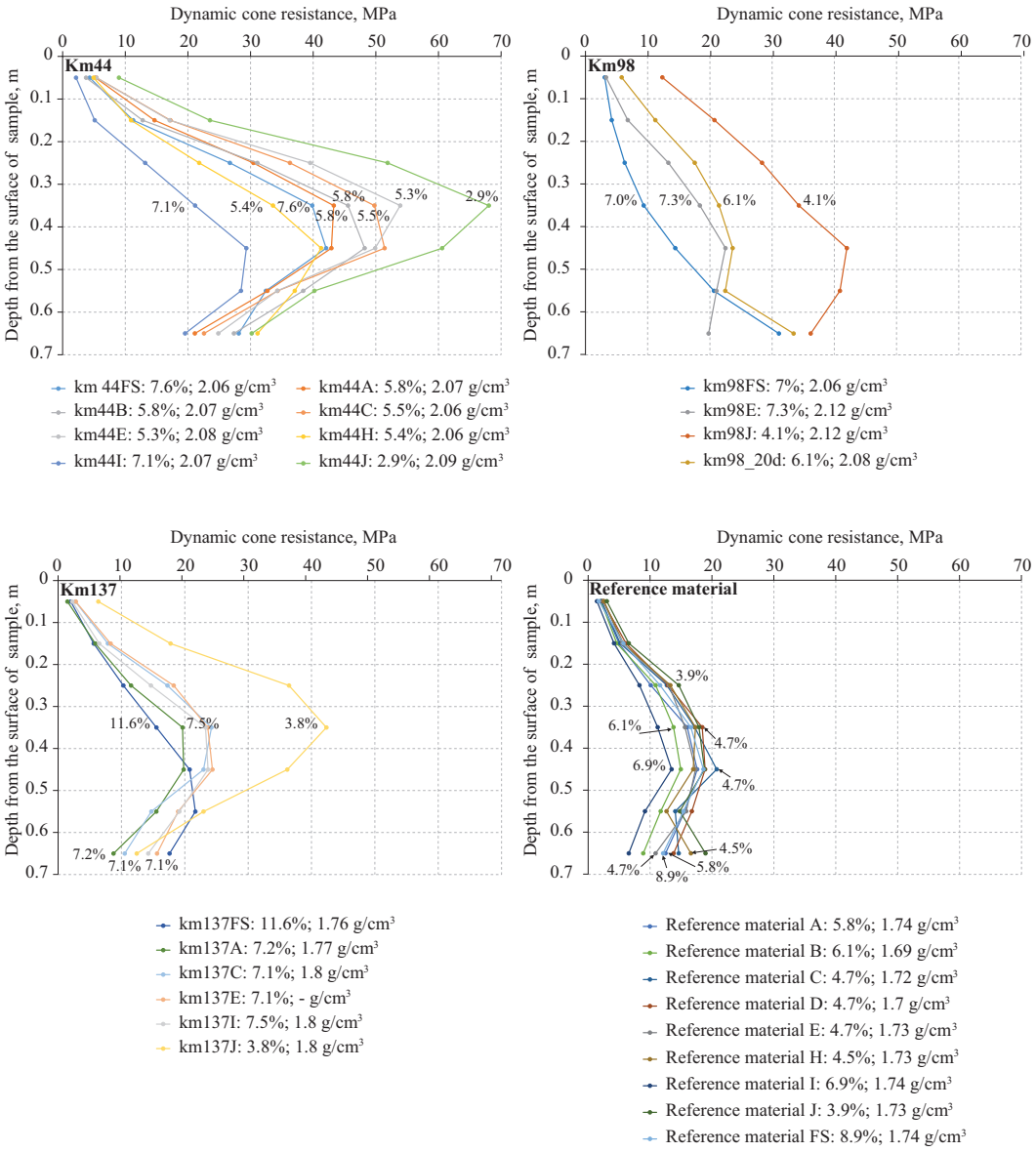

Figure 7. The dynamic cone resistance of entire samples at varying moisture content levels

With moist samples, the dynamic cone resistance varied noticeably according to dry density and moisture content. The moisture content indicates an average across the entire testing depth. The results are

reported in Figure 7, which presents the dynamic cone resistance to depth for the entire sample. The differences among the materials were significant, and the lowest dynamic cone resistance was measured in the reference material, which presented the highest shear strength in static triaxial tests. The highest dynamic cone resistance for all materials was reached at the lowest moisture content level, and the dynamic cone resistance generally decreased with increased moisture content. The results in Figure 7 illustrate the increase in dynamic cone resistance in proportion to depth. Moist samples, too, exhibited similar loosening of the bottom layers as oven-dry samples, but the degree varied depending on the material. Based on the results, the moisture content and dry density in km44 material caused more considerable variation of dynamic cone resistance compared to the reference material, which was the least sensitive to changes in moisture content.

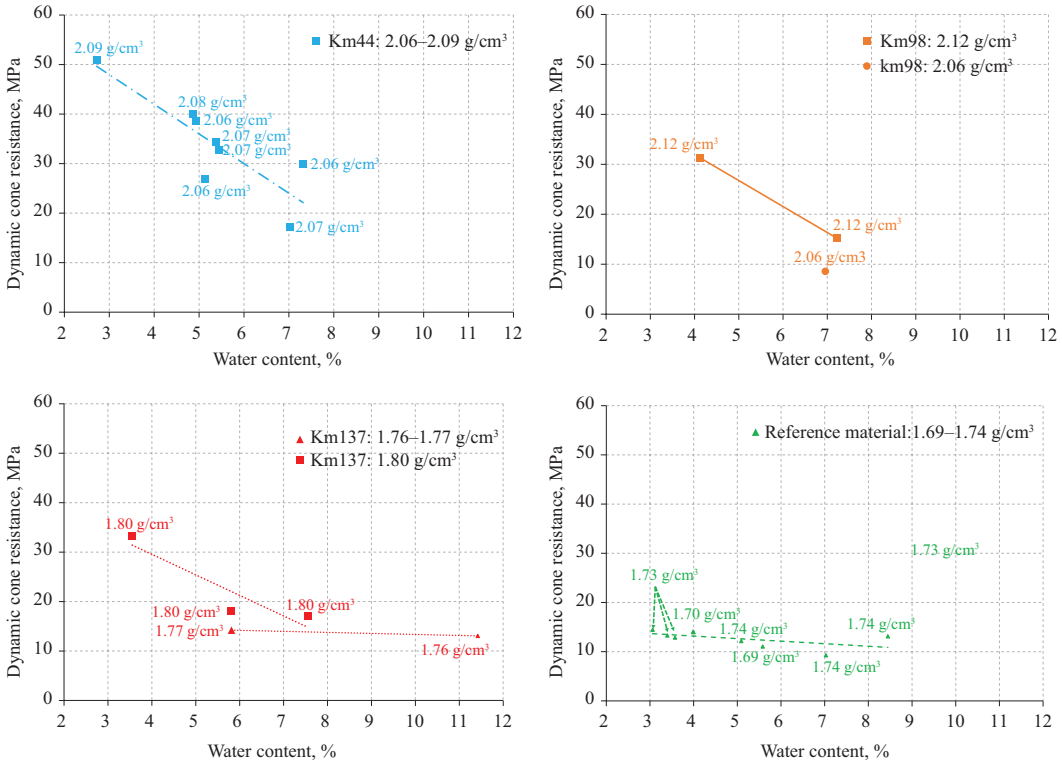

Note: the depth range covered is 0–500 mm.

Figure 8. The impact of moisture content on dynamic cone resistance

A clearer view of the impact of moisture content is provided by Figure 8, in which the dynamic cone resistance is only presented in proportion to moisture content and which only covers a depth of 0–500 mm. This approach excludes the looser bottom section. Figure 8 divides the measuring points into separate categories based on dry density. This method of examination also revealed the reference material to be the least sensitive to increases in moisture content, even though it also exhibited slight growth. The increase is more dramatic with other materials – with km44, for example, the range of variation was above 30 MPa, depending on the dry density and moisture content. As regards material km98 and km137, the dynamic cone resistance increased with decreasing moisture content. The results show similarities with the results of the static triaxial tests, as a moisture content dropping below 7% increases dynamic cone resistance.

3.1. Field measurements

The purpose of the field measurements was to determine the suitability of the device to the Finnish railway environment. The field locations used were sites km44, km98, and km137 along the Rantarata track, at which substructure samples were collected for laboratory testing (at an approximate depth of 0.5 m measured from the bottom surface of the ballast layer). The field surveys were initiated at the km137 point, which is located by a sandy ridge. The substructure was examined near the footpath and on the embankment at various locations, as shown in Figure 9. The most measurements were conducted in this location as the penetrometer rod sank quickly into the soft, even-grained sand. The measured results are presented as a nine-strike average in Figure 10 since these evens out spikes caused by small rocks. The measured dynamic cone resistances were small; approximately equal to 3.0 MPa to a depth of 0.7 m. Because the dynamic cone resistances spiked immediately after that, it was clear that there was either rock or some other material that produced a higher dynamic

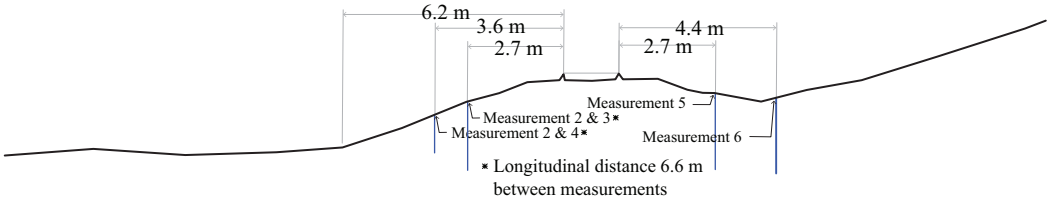

Figure 9. Positions of the Panda tests at the km137 point across a cross-section of the track

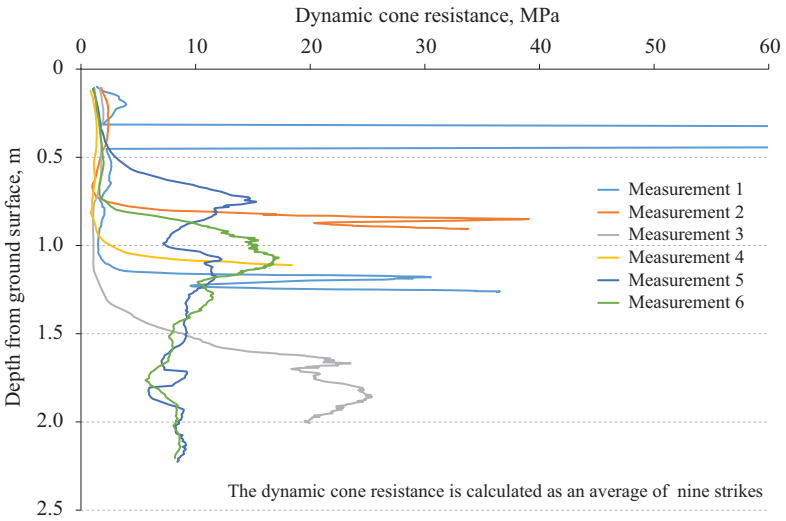

Figure 10. Measurement results for the km137 site

cone resistance below this layer. One measurement hit a rock near the very beginning that caused the peak value shown in the diagram at a depth of approximately equal to 0.4 m. The deepest testing point was 2.2 m. On visual observation, the nearby sandy ridge and the materials used to construct the track mostly resembled each other, and no clear distinctions between layers were identified.

The second field location examined was situated at the km98 point of the Rantarata track. Three measurements were taken at separate locations near the footpath, and the dynamic cone resistances were higher than at the previous km137 location. The results are shown in Figure 11. The dynamic cone resistance for two measurements was approximately equal to 3.0 MPa initially, before beginning an apparent increase at a depth of 1.2 m. For measurement 2, the dynamic cone resistance was immediately higher, but deeper in, the values began to correspond to the other measurements. Two measurements were successful to an approximate depth of 3.5 m, but the third was stopped at 2.0 m due to high resistance. As a technical observation relating to the tests, it was observed that the substructure in this location was more heterogeneous in terms of its particle size and also contained ballast particles. Although the dynamic cone resistance was pretty low, it was challenging to drive the rod into the ground, and long sequences of strikes were needed. The mixed-grained material that also contained ballast particles proved problematic in terms of rod durability.

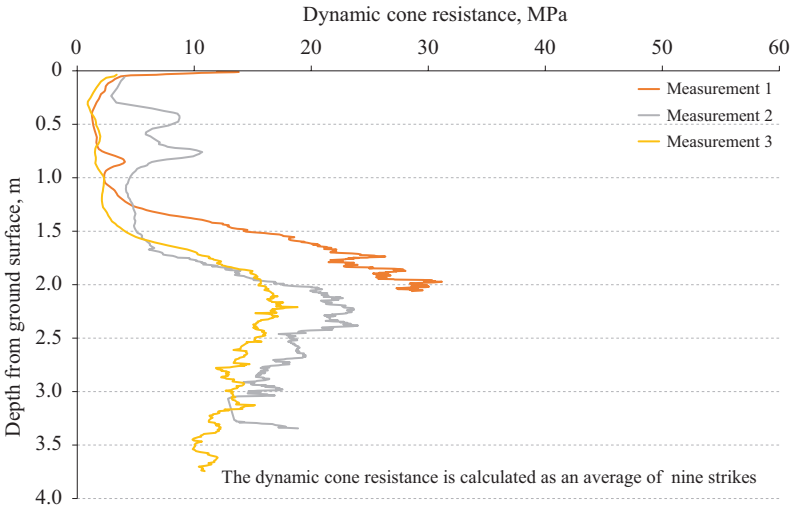

Figure 11. Measurement results for the km98 site

Only one test was conducted at the last test site at the km44 point. The site is situated in a soft soil area, and the track has settled somewhat over the years. The elevation has repeatedly raised with ballast to compensate the settlement. That has caused ballast material to mix with substructure materials. The DCP test was conducted on the footpath outside the actual track to avoid coarse ballast rocks. Despite this, there were significant difficulties to drive the rod into the embankment.

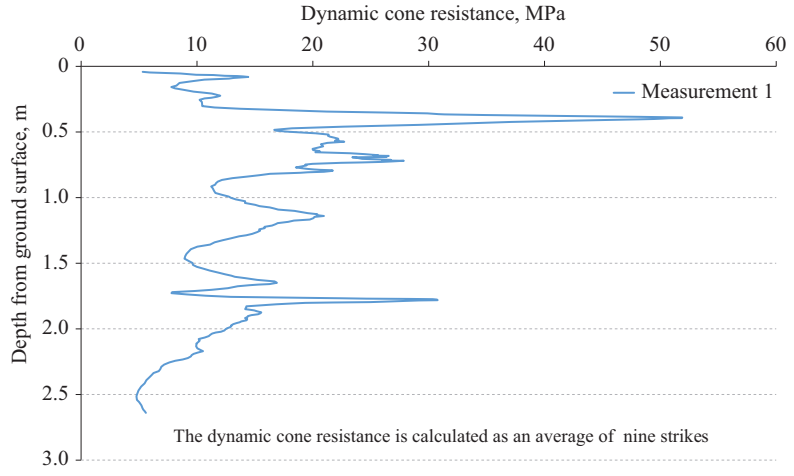

Figure 12. Test results for the km44 site

These difficulties are illustrated well by the results in Figure 12 since the average dynamic cone resistance rose to 10 MPa, relatively near the surface. The dynamic cone resistance increased with depth, and the soil contained rocks that caused spikes to curve. At a depth of 1.7 m, the dynamic cone resistance began to drop, which indicated a softer layer of soil than the substructure. Lifting the rod after the test was also difficult since the rocks encountered in the driving phase caused torsional stress on the rod. Conditions such as those at the site in question require significantly more robust ground surveying equipment.

4. Discussion

The laboratory tests indicated that all materials investigated were different, which was the intention. Based on the triaxial tests, the apparent cohesion present at low moisture content increased the shear strength of the samples examined. For the studied materials, moisture content of approximately equal to 7% appeared to be the turning point, after which the apparent cohesion begins to increase the shear strength. On the other hand, due to the nature of the undrained triaxial tests, the pore water pressure has time to dissipate. At a more rapid cyclic load, the behaviour is partially different. Repeated loading triaxial tests have also been conducted on the materials in question, and the results are presented in an upcoming article.

The Panda2 proved to be a light and easy-to-use DCP device. The series of laboratory tests indicate that the is mostly determined based on the dry density, but the moisture content also has a clear impact. The results have apparent similarities with those published by Escobar, Benz-Navarrete, Gourvès, Haddani, Breul, & Chevalier (2016), wherein a minute increase in the dry density of sand material had a surprisingly strong impact on the dynamic cone resistance measured by the Panda device. This observation is also consistent with other research results, as Chaigneau, Gourves, & Boissier (2000), for example, stated in their article that the dynamic cone resistance measured by DCP is highly sensitive to the effect of dry density. The series of tests showed that the materials brought in from the field (km44, km98, and km137) all clearly reacted to the moisture content. However, the high-quality reference material from Kollola had a relatively low response to the change in moisture content. The link between moisture content and dynamic cone resistance was also observed by Morvan & Breul (2016) in studying silt materials with the Panda device. Byun & Kim (2020) tested their in-situ modulus detector for subgrade and found that the resilient moduli of soil also decreases when the water content increases. That device had

many similarities with DCP. The median particle size of the materials did not appear to affect the dynamic cone resistance in the materials studied substantially. However, the range of particle sizes covered was relatively narrow in this study. The effect of median particle size was also small in the study of MacRobert, Bernstein, & Nchabeleng (2019), when they studied correlations between the relative density of sands and DCP. The standard error in relative density prediction was 11%, but when using median particle size with correlation, the error decreased slightly to 9%.

The dynamic cone resistances measured at the laboratory were significantly higher than those measured in the field. This effect was slightly surprising, but presumably, the plastic tube used expanded during compaction and when driving the rods into the sample. This phenomenon is likely to have caused a confining pressure akin to cell pressure in the material, which increased the resistance required for soil displacement but also resulted in substantial skin resistance affecting the penetrometer rod. Bolton, Gui, Garnier, Corte, Bagge, Laue, & Renzi (1999) had also recognised that cone resistance was above double when ratio (container diameter divided by cone diameter) was decreased from 45 to 8.85. In our test, the ratio was approximately 14. Increased dynamic cone resistance was also observed by Gansonré, Breul, Bacconnet, Benz, & Gourvès (2019) when they tested different boundary conditions with Panda DCP. The dynamic cone resistance in the small chamber was multiple compared to in-situ measurements and more extensive in the small chamber than in the larger one. In our test, materials brought in from the field were excavated by hand from the substructure below the ballast layer. That was the reason why their amount was limited, and the tests were ultimately performed inside a tubular mould. If there had been more materials available, a more extensive and shallower test container would have served the purpose better in hindsight. However, the study unequivocally indicates that skin resistance has a significant impact on the measured values, but the degree is complicated to estimate.

Apparent skin resistance also affected the penetrometer rod in the field tests, especially at the km44 site but also partially at the km98 site. This expectation must be considered in the examination of the results since skin resistance is not taken into account in the calculation of dynamic cone resistance. Using larger sacrificial cones would be a better option, but even the used 2 cm^2 cone proved challenging to drive into the embankment in the field. However, the problem does not appear to occur globally, as Haddani, Breul, Saussine, Navarrete, Ranvier, & Gourvès (2016) have presented measurements taken with the Panda device directly from the top of the ballast

layer in France. In Finnish conditions, it can be concluded that the device lends itself better to measuring the density of various thin layers and surveying softer materials. The same manufacturer is also developing a more heavy-duty measurement device, called Grizzly3, which is stated to be better suited to coarse-grained conditions (Benz-Navarrete, Escobar, Haddani, Gourves, D'Aguiar, & Calon, 2014). However, that is not hand-held instrument anymore, because the newest version of Grizzly EV DPSH has 63.5 kg weight of striking mass and the total mass of testing machine is 990 kg (Benz-Navarrete, Breul, & Moustan, 2019).

The relevant literature presents a variety of solutions for eliminating skin resistance in the DCP device. A method presented by Livneh (2000) where the rod struck at regular intervals, is rotated and the torque this requires is measured to enable the calculation of a corrected dynamic cone resistance value. This method was originally presented by Dahlberg & Bergdahl 1974 (as cited in Livneh, 2000). Abuel-Naga, Holtrigter, & Pender (2011) also present various methods, such as the protective pipe method developed by Meardi & Gadsby 1971. That method involves striking a penetrometer rod into the ground with a large tip, as well as a pipe that protects the penetrometer rod. This trick eliminates friction rather effectively, but fitting the protective pipe presents its own set of problems. The hybrid cone penetrometer, which was developed for evaluating railway substructures (Byun, Hong, & Lee, 2015), also have multiple rods. In that kind of test device, the outer rod is used for penetrating ballast dynamically and then the inner mini cone is used for static penetration of subgrade.

Another method of eliminating skin resistance is the process described by Baudrillard 1974 (as cited in Abuel-Naga, Holtrigter, & Pender, 2011). In that process, drilling fluid is injected into the cavity between the impact rod and the soil to reduce friction significantly. In their article, Abuel-Naga, Holtrigter, & Pender (2011) also present a method they have developed, which is based on raising the impact rod intermittently. In their method, the rod is initially raised by 1 m at the end of the test, after which it is driven back into the ground. The number of strikes required is also measured. Then, the rod is raised by 2 m and driven back in by 1 m. This method enables the measurement of the resistance caused by skin friction only, without the dynamic cone resistance. The precondition for a method of this nature is that the hole formed by the cone remains open for a while. As such, the literature indicates that there are a variety of methods for considering skin friction in a DCP test but, reportedly, they have not been applied to the Panda2 device. Skin friction requires further study before it can be reliably eliminated from the results through compensation.

Based on the laboratory results, identifying low-quality structural materials in field locations is challenging. The dynamic cone resistance measured by a DCP-type device correlates most with the dry density of materials, which does not necessarily correlate with the low bearing capacity of embankment materials. The measured dynamic cone resistance values for the Kollola reference material were low due to the low dry density. However, the km137 material had the same dry density and nearly identical dynamic cone resistance behaviour, even though the materials presented apparent differences in the static triaxial test. The laboratory tests showed that the water content and dynamic cone resistance varied significantly in the vertical sample direction. Presumably, the dry density was slightly lower at the bottom of the sample, judging by the decrease in dynamic cone resistance over the final 200 mm. A large number of variable parameters was problematic for results analysis, which is why only the averages for a 500 mm layer were examined. Based on the difficulties in the implementation of the laboratory tests, it is estimated that the dynamic cone resistance at the field sites is influenced by so many factors that it is practically impossible to identify deficiencies in material quality. Furthermore, estimating the moisture content at field locations in different seasons is nearly impossible due to the presence of too many variables.

The ballast material used in the field locations and particularly in the railway environment caused significant problems to the light device. In old track sections, ballast particles may have sunk into or mixed in with the intermediate and insulating layers, in which case more powerful equipment is needed. The DCP rods used in the device were sensitive to the sideways pull caused by boulders. As such, the device is more suitable for softer soil materials and the density monitoring as marketed by the manufacturer, which does not require long rods and where the material is equal to sand or finer in consistency and even-grained. For road structures, the device is most likely fine, if the material is not coarse-grained crushed rock.

Conclusions

As a device, the dynamic cone penetrometer is quite simple, and Sol Solution has managed to make the Panda2 very easy to use. The lightness of the device is a clear benefit, but it also limits its applications. Based on a comprehensive series of laboratory and field tests, the following responses are provided to the original research questions:

1. A dynamic cone penetrometer type device reacts strongly to the dry density of the material, but moisture content has an impact as

well. However, the results indicate that these parameters are not directly linked to the low bearing capacity of the material, which means that the device cannot be used to identify low-quality substructure materials in railway environments reliably.

2. Drying the sample increased the strength of the material in the triaxial and laboratory tests of a dynamic cone penetrometer. However, field conditions present so many influencing factors that the proportion of moisture content in the test of dynamic cone penetrometer results is likely to not stand out sufficiently among the other factors that have an impact.
3. The light structure of the device is a benefit, but the tests in the railway environment showed that using the device in the vicinity of the ballast layer easily leads to problems. Based on the testing, more robust equipment is required for such environments.

Acknowledgements

Finnish Transport Infrastructure Agency supported this work. Authors are also grateful for research assistant Toni Saarikoski for making the most of Panda2 tests at the laboratory.

Funding

Finnish Transport Infrastructure Agency funded this work.

REFERENCES

Abuel-Naga, H. M., Holtrigter, M., & Pender, M. J. (2011). Simple method for correcting dynamic cone penetration test results for rod friction. *Géotechnique Letters*, *1*(3), 37-40. https://doi.org/10.1680/geolett.11.00012

Benz-Navarrete, M. A., Breul, P., & Moustan, P. (2019, November). Servo-Assisted and Computer-Controlled Variable Energy Dynamic Super Heavy Penetrometer. In *Geotechnical Engineering in the XXI Century: Lessons learned and future challenges: Proceedings of the XVI Pan-American Conference on Soil Mechanics & Geotechnical Engineering (XVI PCSMGE), 17-20 November 2019, Cancun, Mexico* (p. 65). IOS Press.

Benz-Navarrete, M. A., Escobar, E., Haddani, Y., Gourves, R., D'Aguiar, S. C., & Calon, N. (2014). Determination of Soil Dynamic Parameters by the Panda 3®: Railways Platform Case. In *Proc. of the Second International Conference on Railway Technology: Research, Development & Maintenance", Civil-Comp Press, Stirlingshire, UK, Paper* (Vol. 56). https://doi.org/10.4203/ccp.104.56

Bolton, M. D., Gui, M. W., Garnier, J., Corte, J. F., Bagge, G., Laue, J., & Renzi, R. (1999). Centrifuge cone penetration tests in sand. *Géotechnique*, *49*(4), 543-552. https://doi.org/10.1680/geot.1999.49.4.543

Brough, M. J., Ghataora, G. S., Stirling, A. B., Madelin, K. B., Rogers, C. D. F., & Chapman, D. N. (2003, August). Investigation of railway track subgrade. I: In-situ assessment. In *Proc. of the Institution of Civil Engineers-Transport* (Vol. 156, No. 3, pp. 145-154). Thomas Telford Ltd. https://doi.org/10.1680/tran.2003.156.3.145

Brough, M. J., Ghataora, G., Stirling, A. B., Madelin, K. B., Rogers, C. D., & Chapman, D. N. (2006, May). Investigation of railway track subgrade. Part 2: Case study. In *Proc. of the Institution of Civil Engineers-Transport* (Vol. 159, No. 2, pp. 83-92). Thomas Telford Ltd. https://doi.org/10.1680/tran.2006.159.2.83

Byun, Y. H., & Kim, D. J. (2020). In-situ modulus detector for subgrade characterisation. *International Journal of Pavement Engineering*, 1-11. https://doi.org/10.1080/10298436.2020.1743291

Byun, Y. H., Hong, W. T., & Lee, J. S. (2015). Characterisation of railway substructure using a hybrid cone penetrometer. *Journal of Smart Structures & Systems*, *15*(4), 1085-1101. https://doi.org/10.12989/sss.2015.15.4.1085

Chaigneau, L., Gourves, R., & Boissier, D. (2000, February). Compaction control with a dynamic cone penetrometer. In *Proc. of International Workshop on Compaction of Soils, Granulates & Powders, Innsbruck* (pp. 103-109).

Escobar, E., Benz-Navarrete, M. A., Gourvès, R., Haddani, Y., Breul, P., & Chevalier, B. (2016). *Dynamic Characterisation of the Supporting Layers in Railway Tracks Using the Dynamic Penetrometer Panda 3®. Procedia Engineering*, *143*, 1024-1033. https://doi.org/10.1016/j.proeng.2016.06.099

Gansonré, Y., Breul, P., Bacconnet, C., Benz, M., & Gourvès, R. (2019). Prediction of in-situ dry unit weight considering chamber boundary effects on lateritic soils using Panda® penetrometer. *International Journal of Geotechnical Engineering*, 1-7. https://doi.org/10.1080/19386362.2019.1698211

Haddani, Y., Breul, P., Saussine, G., Navarrete, M. A. B., Ranvier, F., & Gourvès, R. (2016). Trackbed Mechanical and Physical Characterisation using PANDA®/ Geoendoscopy Coupling. *Procedia Engineering*, *143*, 1201-1209. https://doi.org/10.1016/j.proeng.2016.06.118

Kennedy, J. (2011). *A full-scale laboratory investigation into railway track substructure performance and ballast reinforcement* (Doctoral dissertation, Heriot-Watt University).

Langton, D. D. (1999). The Panda lightweight penetrometer for soil investigation and monitoring material compaction. *Ground Engineering*.

Lehtonen, I. (2011). *Äärisademäärien muutokset Euroopassa maailmanlaajuisten ilmastomallien perusteella* (in Finish)

Li, D., & Selig, E. T. (1995). Evaluation of railway subgrade problems. *Transportation Research Record*, *1489*, 17-25.

Livneh, M. (2000). Friction correction equation for the dynamic cone penetrometer in subsoil strength testing. *Transportation Research Record*, *1714*(1), 89-97. https://doi.org/10.3141/1714-12

MacRobert, C. J., Bernstein, G. S., & Nchabeleng, M. M. (2019). Dynamic Cone Penetrometer (DCP) Relative Density Correlations for Sands. *Soils & Rocks*, *42*(2), 201-207. https://doi.org/10.28927/SR.422201

Morvan, M., & Breul, P. (2016). Optimisation of in-situ dry density estimation. In *E3S Web of Conferences* (vol. 9, p. 09002). EDP Sciences. https://doi.org/10.1051/e3sconf/20160909002

Ruosteenoja, K., Jylhä, K., & Kämäräinen, M. (2016). Climate projections for Finland under the RCP forcing scenarios. *Geophysica*, *51*.

Scala, A. J. (1956). Simple methods of flexible pavement design using cone penetrometers. *New Zealand Engineering, 11*(2), 34–44.

Selig, E. T., & Waters, J. M. (1994). *Track geotechnology and substructure management*. Thomas Telford.

SFS-EN 13286-2:2011 Unbound and Hydraulically Bound Mixtures. Part 2: Test Methods for Laboratory Reference Density and Water Content. Proctor Compaction

SFS-ISO 17892-9:2018 Geotechnical Investigation and Testing. Laboratory Testing of Soil. Part 9: Consolidated Triaxial Compression Tests on Water Saturated Soils

Spagnoli, G. (2007). An empirical correlation between different dynamic penetrometers. *The Electronic Journal of Geotechnical Engineering*, *12*.

Trenberth, K. E. (2011). Changes in precipitation with climate change. *Climate Research*, *47*(1-2), 123-138. https://doi.org/10.3354/cr00953

Vanags, C., Minasny, B., & McBratney, A. B. (2004, December). The dynamic penetrometer for assessment of soil mechanical resistance. In *Proc. of the 3rd Australian New Zealand Soils Conference* (pp. 5-9).